Mossbauer spectra and magnetic properties of $YTi(Fe_{1-x}Ni_x)_{11}$

1990 J. Phys.: Condens. Matter 2 9621

(http://iopscience.iop.org/0953-8984/2/48/015)

J. Phys.: Condens. Matter 2 (1990) 9621–9629. Printed in the UK

Mössbauer spectra and magnetic properties of $YTi(Fe_{1-x}Ni_x)_{11}$

Z W Li†, X Z Zhou†, A H Morrish† and Y C Yang‡

† Department of Physics, University of Manitoba, Winnipeg, Canada R3T 2N2
‡ Department of Physics, Peking University, Beijing, People's Republic of China

Received 4 July 1990

Abstract. ^{57}Fe Mössbauer spectra and magnetic properties of $YTi(Fe_{1-x}Ni_x)_{11}$ (x = 0–0.6) have been studied. Mössbauer spectra show that the hyperfine fields of the three iron sites and the average hyperfine field increase at first, then decrease and have a maximum between the Ni concentrations $x = 0.2$ and 0.3. The Ni atoms preferentially occupy the 8f site and the Fe atoms the 8i site at Ni concentrations of $x \leq 0.3$ according to the Mössbauer subspectral areas. Magnetic measurements indicate that both the saturation magnetizations at room temperature and the Curie temperatures increase at first and then decrease with Ni substitution. The maximum of the saturation magnetization is 127 emu g^{-1} at a Ni concentration of $x = 0.1$ and that of the Curie temperature is 602 K at $x = 0.3$. The concentration dependences of the saturation magnetizations and the Curie temperatures are calculated using $M_s = 11[(1-x)\mu_{Fe} + x\mu_{Ni}]$ and $T_f = (1/2N)\{n_{Fe-Fe}T_{Fe-Fe} + n_{Ni-Ni}T_{Ni-Ni} + [(n_{Fe-Fe}T_{Fe-Fe} - n_{Ni-Ni}T_{Ni-Ni})^2 + 4n_{Fe-Ni}n_{Ni-Fe}T^2_{Fe-Ni}]^{1/2}\}$, respectively. The results obtained are in accord with the experimental data.

1. Introduction

In recent years, much work [1–4] has been reported on the magnetic properties of $RFe_{12-x}M_x$ (R is a rare-earth atom and M denotes Ti, Mo, V, Si and W) because of their probable applications as permanent magnets. $RFe_{12-x}M_x$ compounds have a $ThMn_{12}$ crystal structure belonging to the space group I4/mmm where the 3d atoms locate on the 8i, 8j and 8f sites and rare earth atoms on the 2a site. These compounds, such as $SmTiFe_{11}$, have a high uniaxial magnetocrystalline anisotropy. The origin is mainly the R atoms but the Fe atoms also play an important contribution. The fairly high saturation magnetization and magnetic ordering temperature are mainly attributed to the moment of the 3d atoms and the 3d–3d exchange interaction, respectively. Hence, it is necessary to study the effect of 3d atoms on the magnetic properties in order to achieve the goal of choosing a good permanent magnet.

We concentrate our interest on the 3d magnetism of $YTiFe_{11}$. In a previous paper [5], Mössbauer studies of $YTiFe_{11}$ showed that the order of the magnitude of the hyperfine fields is $H_{hf}(8i) > H_{hf}(8j) > H_{hf}(8f)$ and that the Ti atoms occupy the 8i site. In this paper we study the Mössbauer spectra of $YTi(Fe_{1-x}Ni_x)_{11}$ (x = 0–0.6) to determine the hyperfine fields and the occupancy of the Ni atoms on the three 3d sites. Meanwhile, the concentration dependence of the saturation magnetization and Curie temperature has also been studied and discussed.

0953-8984/90/489621+09$03.50

2. Experiment

The samples were prepared by arc-melting of better than 99.5% pure primary materials in a purified argon atmosphere, followed by annealing at about 1100 K for four hours in vacuum and then quenching in air. The compositions of the samples are $YTi(Fe_{1-x}Ni_x)_{11}$ with $x = 0$, 0.1, 0.2, 0.3, 0.4 and 0.6. X-ray diffraction showed that all samples were a single phase with the $ThMn_{12}$ structure except for $YTi(Fe_{0.4}Ni_{0.6})_{11}$ which had a small amount of an impurity phase.

^{57}Fe Mössbauer spectra of $YTi(Fe_{1-x}Ni_x)_{11}$ were taken at room temperature using a conventional constant-acceleration spectrometer. The γ-ray source was ^{57}Co in a Rh matrix. Mössbauer absorbers were powdered samples with about 10 mg cm^{-2} of natural iron. The calibration was made by using the spectrum of α-Fe at room temperature. The Curie temperatures were obtained by using the Mössbauer thermal scan method. The saturation magnetizations were measured with a vibrating sample magnetometer in applied fields up to 2 T at room temperature.

Mössbauer spectra of $YTi(Fe_{1-x}Ni_x)_{11}$ were analyzed using four sextets with Lorentzian line shapes. Some constraints were used in the fitting procedure. The quadrupole interaction was treated as a perturbation on the magnetic-dipole interaction. The area ratios of the six absorption lines in each sextet were assumed to be $3 : b : 1 : 1 : b : 3$, where b was a fitted parameter. The value of b was about 2.0 for all samples with the exception of $YTi(Fe_{0.4}Ni_{0.6})_{11}$ for which $b \simeq 2.6$. A possible reason for such a high value of b for $YTi(Fe_{0.4}Ni_{0.6})_{11}$ was the magnetic texture in the absorber. However, since rotation the absorber from 90° to 45° with respect to the γ-ray direction did not lead to any significant change of b, the texture effect seems to be ruled out. The cause for such an unusual value of b is unclear and will need to be investigated further. The linewidths of the first and sixth, the second and fifth and the third and fourth peaks of each subspectrum were about $0.6 \sim 0.7, 0.5 \sim 0.6$ and 0.3 mm s^{-1} respectively. The broading of the lines could be attributed to the distribution of Ti and Ni atoms adjacent to each site. The singlet line in $YTi(Fe_{0.4}Ni_{0.6})_{11}$ corresponded to the impurity phase.

3. Results and discussion

3.1. Mössbauer spectra

Figure 1 shows the ^{57}Fe Mössbauer spectra of $YTi(Fe_{1-x}Ni_x)_{11}$ ($x = 0$–0.6) observed at room temperature. In the figure the points indicate the experimental spectra and the full curves represent the fitted curves obtained by computer analysis. Two subspectra are assigned to the 8i site and the other two to the 8j and 8f sites, respectively; these assignments are based on the results of $YTiFe_{11}$ [5]. The fitted Mössbauer parameters are listed in table 1.

The average quadrupole splittings have a slight decrease with Ni substitution, changing from 0.11 mm s^{-1} for $x = 0$ to 0.03 mm s^{-1} for $x = 0.6$. The average isomer shifts rise to -0.07 mm s^{-1} for $x = 0.6$ from -0.19 mm s^{-1} for $x = 0$. This behaviour is attributed to an increase in the 3d electrons, which enhances the shielding of the 4s electrons and thus decreases the charge density at the nucleus.

As shown in figure 2, the hyperfine fields H_{hf} of all three sites increase with Ni substitution at first and then decrease; a maximum occurs between $x = 0.2$ and 0.3. Figure 3 shows the concentration dependence of the average hyperfine field $\langle H_{hf} \rangle$ in

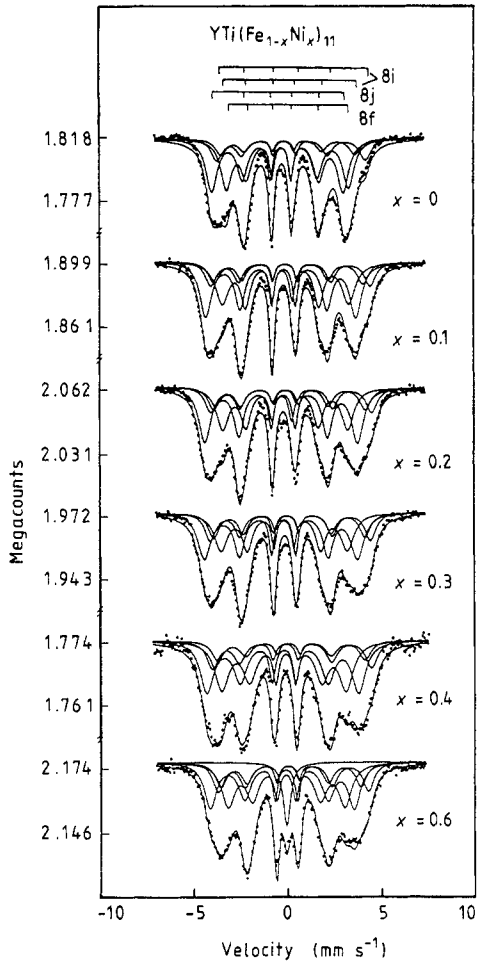

Figure 1. Mössbauer spectra of $YTi(Fe_{1-x}Ni_x)_{11}$ and computer-fitted curves.

$YTi(Fe_{1-x}Ni_x)_{11}$. For comparison, similar plots for other R–(Fe, Ni) compounds have been also shown in figure 3 [6, 7]. The similarity of the curves is striking. This behaviour can be described on the basis of a rigid-band model.

With increasing Ni concentration, the subspectral areas for the 8j site only change a little. However, the areas for the 8f site decrease from 35.6 % for $x = 0$ to a minimum of 29.4 % for $x = 0.3$ and then increase to 34.3 % for $x = 0.6$ and the areas for the 8i site increase to a maximum of 34.6 % for $x = 0.3$ and then decrease. This behaviour shows that the Ni atoms have a preference for certain sites. If it is assumed that the free-recoil fractions on the three sites are the same, the occupation numbers N_i(Fe) and N_i(Ni) of Fe and Ni atoms on the three sites in $YTi(Fe_{1-x}Ni_x)_{11}$, can be estimated by the following formulae:

$$N_i(\mathrm{Fe}) = 11\frac{C_1}{C_1 + C_2}\frac{S_i}{\sum_{i=1}^{3} S_i} \tag{1}$$

$$N_i(\mathrm{Ni}) = N_i - N_i(\mathrm{Fe}) - N_i(\mathrm{Ti}) \tag{2}$$

where C_1 and C_2 denote the atomic compositions of Fe and Ni, N_i is the occupation numbers of the ith 3d site and S_i is the area of the ith subspectrum of $YTi(Fe_{1-x}Ni_x)_{11}$.

Table 1. Hyperfine parameters of $YTi(Fe_{1-x}Ni_x)_{11}$. H_{hf}, hyperfine field; ϵ, quadrupole splitting; δ, isomer shift (relative to the α-Fe at room temperature) and S, relative area.

x	Site	H_{hf}(T)	ϵ (mm s^{-1})	δ (mm s^{-1})	S (%)
	8i	23.6	0.31	0.01	26.8
0	8j	21.8	−0.16	−0.35	37.6
	8f	20.2	0.27	−0.16	35.6
	8i	25.5	0.24	0.03	29.6
0.1	8j	24.8	−0.14	−0.28	38.0
	8f	20.9	0.18	−0.16	32.5
	8i	25.8	0.27	0.07	31.5
0.2	8j	25.3	−0.10	−0.23	38.3
	8f	21.1	0.17	−0.16	30.2
	8i	25.8	0.23	0.09	34.6
0.3	8j	25.3	−0.15	−0.25	36.0
	8f	20.9	0.15	−0.14	29.4
	8i	25.5	0.27	0.10	30.4
0.4	8j	25.1	−0.16	−0.22	36.3
	8f	20.4	0.12	−0.13	33.4
	8i	24.0	0.21	0.14	29.7
0.6	8j	23.7	−0.21	−0.21	35.9
	8f	19.3	0.12	−0.10	34.3

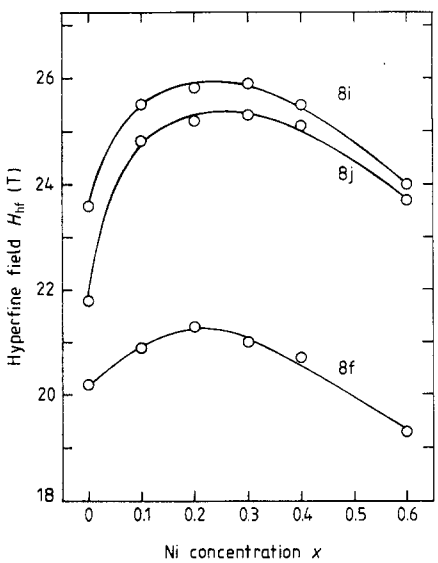

Figure 2. Concentration dependence of the hyperfine fields of the three inequivalent sites in $YTi(Fe_{1-x}Ni_x)_{11}$ at room temperature.

N_i(Ti) are the occupation numbers of the Ti atoms, which are considered to occupy the 8i site only [5]. The results are shown in figure 4. At an Ni concentration $x \leq 0.3$, Ni atoms preferentially occupy the 8f site, Fe atoms preferentially occupy 8i site, and the Fe and Ni atoms occupy the 8j site in proportion to their concentrations. At $x > 0.3$, both Ni and Fe atoms have no site preferences.

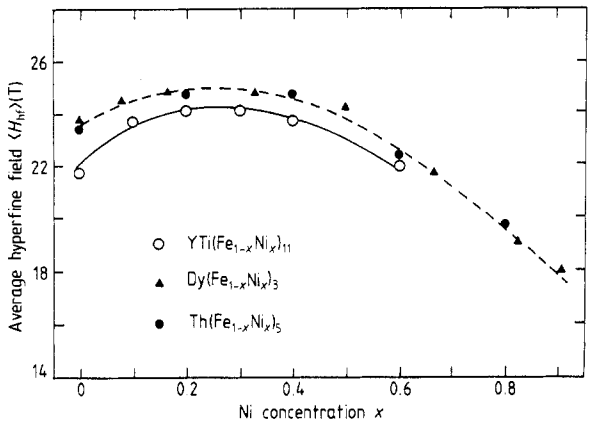

Figure 3. Concentration dependence of the average hyperfine fields of $YTi(Fe_{1-x}Ni_x)_{11}$ at room temperature. The data for $Th(Fe_{1-x}Ni_x)_5$ at 5 K [6] and $Dy(Fe_{1-x}Ni_x)_3$ at 4.2 K [7] are also shown.

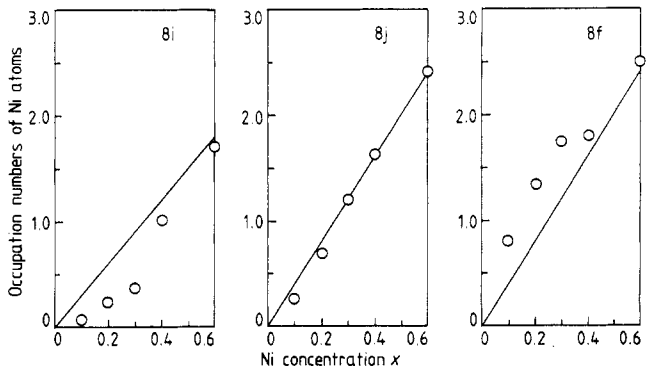

Figure 4. The occupation numbers of Ni atoms on the three 3d sites. The full lines indicate a non-preferential occupation.

Table 2. The saturation magnetizations at room temperature and the Curie temperatures for $YTi(Fe_{1-x}Ni_x)_{11}$.

x	0	0.1	0.2	0.3	0.4	0.6
M_s(emu g^{-1})	123	127	115	109	96	72
$M_s(\mu_B/FU)$	16.3	16.9	15.4	14.7	13.2	9.8
T_f(K)	525	550	580	602	596	566

3.2. Magnetic properties

The magnetic properties of $YTi(Fe_{1-x}Ni_x)_{11}$ are listed in table 2. The saturation magnetizations M_s were found by fitting the experimental data of $M(H)$ against H using the law of approach to saturation

$$M(H) = M_s[1 - (a/H) - (b/H^2)] \tag{3}$$

where $M(H)$ is the magnetization at the magnetic field H after consideration of the demagnetizing field. The saturation magnetizations have a maximum at the Ni concentration $x = 0.1$, which is similar to the result of Yang *et al* at 1.5 K [8].

In Y–Fe compounds the average hyperfine field is proportional to the average magnetic moment of the Fe atoms, as shown in figure 5. The slope of the straight line is 14.5 T/μ_B, as calculated by the least-squares method. The average moment of the Fe atoms in $YTi(Fe_{1-x}Ni_x)_{11}$ has been derived from the average hyperfine field by using this coefficient; the results are shown in figure 6(*a*). If it is assumed that the moment of an Ni atom is 0.6 μ_B, the saturation magnetizations M_s in $YTi(Fe_{1-x}Ni_x)_{11}$ are predicted to be

$$M_s = 11[(1-x)\mu_{Fe} + x\mu_{Ni}]. \tag{4}$$

The results obtained are also shown in figure 6(*b*). They are in reasonable agreement with the experimental data.

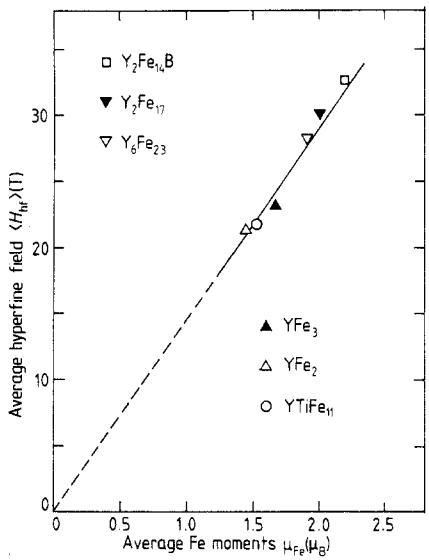

Figure 5. The average hyperfine fields vs the corresponding average Fe moments. Data for Y_xFe_y and $Y_2Fe_{14}B$ are taken from [9] and [10] respectively. The full curve is obtained by the least-squares method; the slope is 14.5 T/μ_B.

The Curie temperature for $YTiFe_{11}$ is $T_f = 525$ K, increases to a maximum of 602 K for $x = 0.3$ and then decreases with increasing Ni substitution, as shown in figure 7. This behaviour is markedly different from some other R–(Fe,Ni) compounds, in which the Curie temperature either decreases monotonically and rapidly with increasing Ni concentration, as for $Th(Fe,Ni)_5$ [6] and $Dy(Fe,Ni)_3$ [7], or slightly increases, as for $Y_2(Fe,Ni)_{14}B$ [11].

In the mean-field approximation in binary alloys proposed by Kouvel [12], the Curie temperatures T_f of $YTi(Fe_{1-x}Ni_x)_{11}$ can be deduced to be

$$T_f = \frac{1}{2N}\{n_{Fe-Fe}T_{Fe-Fe} + n_{Ni-Ni}T_{Ni-Ni} + [(n_{Fe-Fe}T_{Fe-Fe} - n_{Ni-Ni}T_{Ni-Ni})^2 + 4n_{Fe-Ni}n_{Ni-Fe}T^2_{Fe-Ni}]^{1/2}\} \tag{5}$$

where n_{Fe-Fe} and n_{Fe-Ni} are the average numbers of the nearest-neighbour Fe and Ni atoms around an Fe atom, respectively, n_{Ni-Fe} and n_{Ni-Ni} are those around an Ni

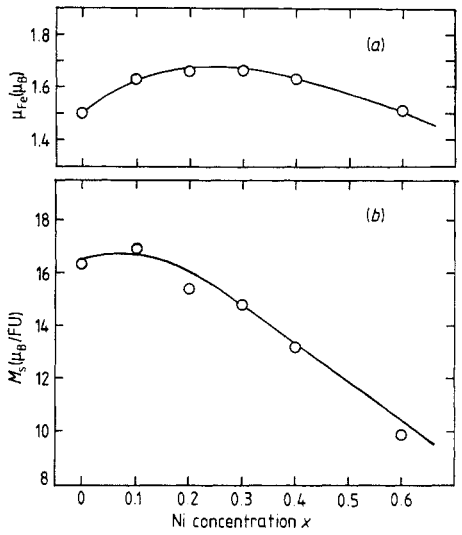

Figure 6. (*a*) The average moment of Fe atoms and (*b*) the saturation magnetizations in $YTi(Fe_{1-x}Ni_x)_{11}$. The full curve is obtained from formula (4), where the Fe moments come from (*a*) and the Ni moment is assumed to be 0.6 μ_B.

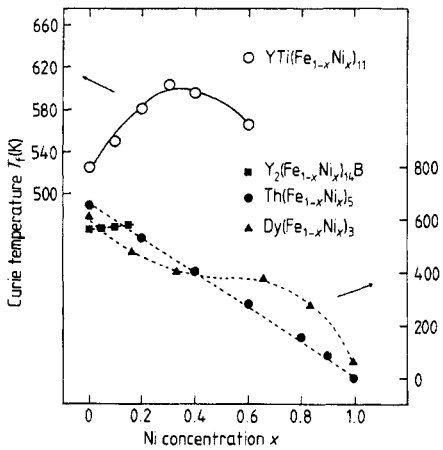

Figure 7. Concentration dependence of the Curie temperatures in $YTi(Fe_{1-x}Ni_x)_{11}$. The full curve is the fitted curve in the mean-field approximation. Concentration dependences of the Curie temperatures in $Y_2(Fe_{1-x}Ni_x)_{14}B$ [12], $Th(Fe_{1-x}Ni_x)_5$ [6] and $Dy(Fe_{1-x}Ni_x)_3$ [7] are also shown.

atom, respectively, N is the total average number of the nearest neighbour Fe plus Ni atoms and T_{Fe-Fe}, T_{Fe-Ni} and T_{Ni-Ni} are the exchange temperatures for Fe–Fe, Fe–Ni and Ni–Ni atoms respectively. These temperatures represent the magnitude of the exchange interactions between the atoms and are given by

$$\begin{aligned} T_{Fe-Fe} &= [(S+1)/6Sk]N\mu_{Fe}^2 J_{Fe-Fe} \\ T_{Ni-Ni} &= [(S+1)/6Sk]N\mu_{Ni}^2 J_{Ni-Ni} \\ T_{Fe-Ni} &= [(S+1)/6Sk]N\mu_{Fe}\mu_{Ni} J_{Fe-Ni} \end{aligned} \tag{6}$$

where k is the Boltzmann constant, S is the spin-quantum number (taken as $\frac{1}{2}$), μ_{Fe} and μ_{Ni} are the magnetic moments of the Fe and Ni atoms and J_{Fe-Fe}, J_{Ni-Ni} and J_{Fe-Ni} are the exchange integrals for Fe–Fe, Ni–Ni and Fe–Ni atom pairs.

The experimental data for the Curie temperatures were fitted by using equation (5), where T_{Fe-Fe}, T_{Fe-Ni} and T_{Ni-Ni} were taken as fitting parameters. The values for n_{Fe-Fe}, n_{Fe-Ni}, n_{Ni-Fe} and n_{Ni-Ni} were obtained from the distribution of Fe and Ni atoms on the three sites and analysis of the neighbouring coordinations for the three sites in $ThMn_{12}$ structure; N was calculated to be 8.94. From the fit, T_{Fe-Fe}, T_{Fe-Ni} and T_{Ni-Ni} are 521 K, 735 K and 345 K, respectively. The fitted curve, as shown by the full curve in figure 7, is in reasonable agreement with experiment. Hence, the mean-field approximation predicts the concentration dependence of the Curie temperatue quite well; meanwhile we come to the conclusion that the exchange interaction for an Fe–Ni pair is stronger than those for Fe–Fe and Ni–Ni pairs in $YTi(Fe_{1-x}Ni_x)_{11}$. This feature is somewhat similar to Ni–Fe alloys, in which the corresponding T_{Fe-Ni}, T_{Ni-Ni} and T_{Fe-Fe} temperatures are 1400, 651 and −170 K respectively [12] and to some amorphous alloys, such as $(Fe, Ni)_{80}B_{20}$ and $(Fe, Ni)_{80}P_{14}B_6$, in which T_{Fe-Ni} is again larger than T_{Fe-Fe} and T_{Ni-Ni} [13].

On the other hand, Yang *et al* [8] proposed a different model for the concentration dependence of the Curie temperature in $YTi(Fe_{1-x}Ni_x)_{11}$. The distance of an 8f–8f atom pair is only 2.390 Å. With such a short distance, reduced magnetic interactions or even negative interactions are possible. The increase of the Curie temperature by the substitution of Fe with Ni can occur if Ni atoms prefer 8f sites. The results of our Mössbauer spectra show that Ni atoms indeed do occupy the 8f sites preferentially.

4. Conclusion

We summarize our main results about $YTi(Fe_{1-x}Ni_x)_{11}$.

(i) The hyperfine fields of the three sites and the average hyperfine field increase at first, then decrease with increasing x and have a maximum between Ni concentrations of $x = 0.2$ and 0.3.

(ii) Ni atoms preferentially occupy the 8f site and Fe atoms the 8i site for $x \leq 0.3$.

(iii) Both the saturation magnetizations at room temperature and the Curie temperatures increase first and then decrease with increasing Ni substitution. The maximum of the saturation magnetization is 127 emu g^{-1} at the Ni concentration $x = 0.1$ whereas the maximum of the Curie temperature is 602 K at $x = 0.3$.

References

[1] De Bore F R, Huang Ying-kai, De Mooij D B and Buschow K H J 1987 *J. Less-Common. Met.* **135** 189
[2] De Mooij D B and Buschow K H J 1988 *J. Less-Common. Met.* **136** 207
[3] Buschow K H J 1988 *J. Appl. Phys.* **63** 3130
[4] Coey J M D 1989 *J. Magn. Magn. Mater.* **80** 9
[5] Li Z W, Zhou X Z, Morrish A H and Yang Y C 1990 *J. Phys.: Condens. Matter* **2** 4253
[6] Van Diepen A M, Buschow K H J and Van Wieringen J S 1972 *J. Appl. Phys.* **43** 645
[7] Tsai S C, Narasimhan K S V L, Kunesh C J and Butera R A 1974 *J. Appl. Phys.* **45** 3582
[8] Yang Y C, Sun Hong, Zhang Z Y, Luo Tong and Gao J L 1988 *Solid State Commun.* **68** 175
[9] Gubbens P C M, Van Apeldoorn J H F, Van der Kraan A M and Buschow K H J 1974 *J. Phys. F: Metal Phys.* **4** 921

[10] Van Noort H M, De Mooij D B and Buschow K H J 1985 *J. Appl. Phys.* **57** 5414
[11] Lin Chin, Lan Jian and Xu Xiao-Feng 1987 *J. Appl. Phys.* **61** 3457
[12] Kouvel J S 1969 *Magnetism and Metallurgy* vol 2, ed A E Berkowitz and E Kneller (New York: Academic) pp 523–75
[13] Becker J J, Luborsky F E and Walter J L 1977 *IEEE Trans. Magn.* **MAG-13** 988